Journal of Luminescence 130 (2010) 87–91

Contents lists available at ScienceDirect

Journal of Luminescence

journal homepage: www.elsevier.com/locate/jlumin

Light emission from nanocrystalline silicon clusters embedded in silicon dioxide: Role of the suboxide states

Andriy Romanyuk [a,*], Viktor Melnik [b], Yaroslav Olikh [b], Johannes Biskupek [c], Ute Kaiser [c], Martin Feneberg [d], Klaus Thonke [d], Peter Oelhafen [a]

[a] Department of Physics, University of Basel, 4056 Basel, Switzerland
[b] Institute of Semiconductor Physics, 03028 Kyiv, Ukraine
[c] Electron Microscopy Group of Materials Science, University of Ulm, 89069 Ulm, Germany
[d] Institute of Semiconductor Physics, University of Ulm, 89081 Ulm, Germany

ARTICLE INFO

Article history:
Received 23 March 2009
Received in revised form
21 June 2009
Accepted 28 July 2009
Available online 5 August 2009

PACS:
61.46.+w
73.20.−r
78.67.−n
79.60.Jv
81.07.−b

Keywords:
Silicon nanoclusters
Photoluminescence
Cluster–matrix interface
Ultrasound

ABSTRACT

Silicon clusters embedded in a silicon dioxide matrix were prepared by ultrasound-assisted implantation resulting in a modified concentration of suboxide states as revealed by high-resolution photoelectron spectroscopy. It is suggested that ultrasound treatment results in formation of different interface structure between silicon cluster and silicon dioxide matrix which is characterized by a distinctly reduced concentration of the suboxide states. It is observed that photoluminescence properties are strongly correlated with the concentration of the suboxide states thereby providing an evidence that besides a quantum confinement effect a closer look at the chemical composition of the nc-Si/SiO_2 system is important.

© 2009 Elsevier B.V. All rights reserved.

1. Introduction

Silicon is an indirect band gap semiconductor with the lowest point of the conduction gap shifted from the center of the Brillouin zone resulting in poor efficiency of light emission. Since the first observation of visible photoluminescence from porous silicon at room temperature reported in 1990 by Canham [1,2], properties of low dimensional silicon quantum structures have been a subject of extensive investigations motivated by the broad potential application of nanosized silicon in photonic and optoelectronic devices (for review see Refs. [3,4]). A large amount of work on the light emission from silicon-based nanostructures have been published so far with the majority devoted to the optical properties of nanocrystalline silicon (nc-Si) clusters embedded in the dielectric matrix of silicon dioxide.

Some of the most fundamental questions related to the mechanism of light emission from silicon nanocrystals are still a matter of debate. On the one hand it is widely believed that the indirect gap limitation is surmounted by confinement of the exciton wave function in silicon crystallites with size below the size of the free exciton Bohr radius which is equal 4.3 nm for bulk silicon [5,6]. In this case, the increase in the overlap of the electron and the hole wave functions substantially increases the probability of a radiative recombination process resulting in higher luminescence efficiency. On the other hand, the light emission could also be due to the recombination via defect levels localized on the interface between nanocrystal and the amorphous silicon oxide matrix [7,8]. Several models of the interface-mediated light emission have been suggested including distortion of surface geometry [9], formation of pinning states [10,11], or assistance of a Si–O bond vibration at the nc-Si/SiO_2 interface [12].

The silicon nanocrystals can be produced by annealing silicon oxide supersaturated with excess silicon atoms, either introduced during growth by sputtering [13,14], chemical vapor deposition [15,16], laser ablation [17], or by ion implantation [18,19]. The latter method is routinely used in silicon integrated circuit technology and offers a number of advantages such as high controllability of dopant concentration and spatial distribution, as

* Corresponding author. Tel.: +41 61 267 37 20; fax: +41 61 267 37 84.
E-mail address: andriy.romanyuk@unibas.ch (A. Romanyuk).

0022-2313/$ - see front matter © 2009 Elsevier B.V. All rights reserved.
doi:10.1016/j.jlumin.2009.07.021

well as the possibility of extending elemental clusters forming compounds using sequential implantation of different ions. Recently we presented a new approach to cluster engineering by implanting ions in silicon oxide with ultrasound vibrations applied *in situ*, i.e. during the ion implantation process [20,21]. It has been shown that *in situ* applied ultrasonic treatment during implantation of silver or copper leads to the lowering of the metal precipitation threshold and an increase in precipitate size after post-implantation annealing. The physical mechanism of this effect was attributed to the enhanced diffusion of metal atoms stimulated by accumulation of vacancies in the precipitation region. Our study on the influence of *in situ* applied acoustic waves on oxidation of tungsten in oxygen plasma demonstrated a formation of a distinctly sharper WO–W planar interface as opposed to the normal oxidation [22]. It was then expected that the ultrasonic treatment resulted in a different concentration of interfacial suboxide states. Although the data on planar WO–W interface cannot be directly transferred to the case of nc-Si/SiO_2 interface for a number of obvious reasons, it is conceivable that implantation of silicon ions with *in situ* applied ultrasound might result in a modified structure of the Si-cluster/SiO_2-matrix interface as compared to normal implantation. The comparison of optical properties of silicon clusters of the same size but with a different structure of cluster/matrix interface might give an answer to the question of the radiative recombination mechanism in nanosized silicon.

Here we demonstrate that applied ultrasound vibrations lead to reduced concentration of suboxide states after post-implantation annealing as compared to the normally implanted samples, i.e. samples prepared without ultrasound treatment. It is suggested that the suboxide states are originated from the interface between silicon cluster and silicon dioxide matrix thereby presenting an unique system for revealing the role of the interface structure in the light emission. We found a strong correlation between the concentration of suboxide states and optical properties of nc-Si/SiO_2 systems thus necessitating careful consideration of the system chemistry when optical properties are of concern.

2. Experimental details

Boron-doped (1 0 0) silicon wafers covered with 600 nm thermally grown oxide were implanted with 100 keV silicon ions at a dose of $8 \times 10^{16}\,cm^{-2}$ keeping the ion flux constant at $2.0 \times 10^{12}\,cm^{-2}\,s^{-1}$. The ultrasound vibrations were generated in the sample during the implantation process by an a.c. driven piezoelectric transducer operating in resonance vibration mode at a frequency of 9.5 MHz and an acoustic power of $0.3-1.0\,W\,cm^{-2}$. The corresponding elastic mechanical deformation was estimated to be 2×10^{-6} to 4×10^{-6}, respectively. The sample was spring-pressed directly onto the ultrasound transducer and acoustic waves were propagating orthogonal to the sample surface. The samples temperature during the implantation process was controlled by a *K*-type thermocouple and did not exceed 50 °C. The samples were finally annealed in a nitrogen atmosphere at 1100 °C for 40 min.

A HeCd laser operating at a wavelength of 325 nm and power of 30 mW was used for the excitation of steady-state photoluminescence. Photoluminescence spectra were recorded at room temperature by a liquid nitrogen cooled charge-coupled device camera mounted on a grating monochromator. Thin cross

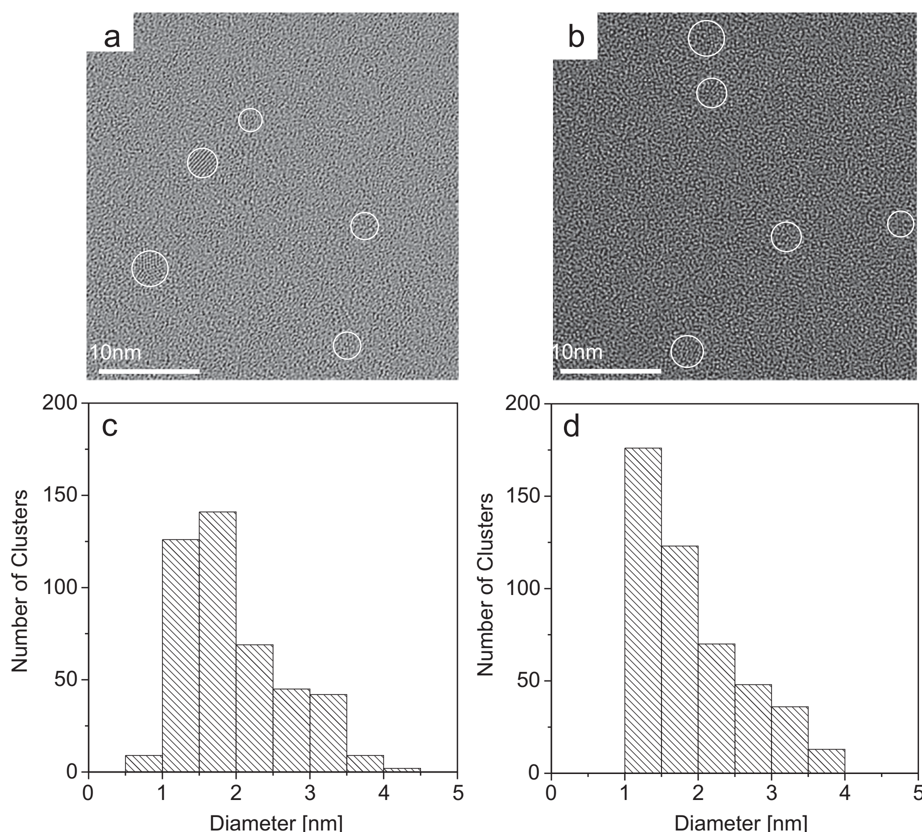

Fig. 1. High-resolution TEM micrographs of silicon clusters prepared by ion implantation of silicon at a dose of $8 \times 10^{16}\,cm^{-2}$ (a) without and (b) with applied ultrasound at acoustic power of $1.0\,W/cm^2$. Annealing 1100 °C for 40 min in N_2. The silicon clusters are marked with white dotted circles. (c) and (d) represent the corresponding histograms of the size distribution obtained by analysis on the bright-field STEM images.

sectional transmission electron microscope (TEM) samples before and after the high-temperature annealing step were prepared. This was done by cutting and gluing of sandwich stripes followed by mechanical grinding, polishing and low angle Ar^+ ion beam etching (8°, 1–4 kV). The synthesized Si nanoparticles were structurally characterized by an FEI Titan 80−300 C_S-corrected transmission electron microscope (TEM) operating at 300 kV.

In order to make the silicon particles accessible for analysis by photoelectron spectroscopy, the samples with embedded nanoclusters were stepwise treated in a buffered solution of hydrofluoric acid (BHF) resulting in an effective etching of silicon dioxide and leaving a hydrogen-terminated silicon surface [23,24]. The hydrogen was then removed by heating the samples in vacuum at 500 °C and the specimens were transferred into the analysis chamber of the electron spectrometer without breaking the vacuum. The photoelectron spectra were recorded using a VG ESCALAB 210 system equipped with a monochromatized Al*K*α (1486.6 eV) radiation source with an overall resolution of 0.32 eV. Charge compensation was done with a flood-gun. The energy calibration of the spectrometer has been performed by setting the $4f_{7/2}$ core level binding energy of a clean gold sample at 84.0 eV.

3. Results and discussion

Fig. 1 shows high-resolution bright field TEM images taken on normally implanted (a) and with *in situ* applied ultrasound (b) samples together with corresponding cluster size distributions ((c) and (d)). The silicon nanocrystallites of a spherical shape are clearly distinguished from the amorphous matrix in high resolution imaging mode due to their periodic lattice (phase contrast). The average particle size was found to be 1.92 ± 0.7 and 1.97 ± 0.7 nm for samples implanted without and with applied ultrasound, respectively. Analysis of dark-field scanning TEM images (not presented here) reveals that in-depth distribution of silicon particles are closely similar in both samples with centroid located near 130 nm, near to the silicon implantation projected range (R_p).

Fig. 2 illustrates the Si-2p spectra acquired at the depth of the maximum cluster distribution in the normally implanted sample (top spectrum) and in the sample implanted with applied ultrasound (bottom spectrum). The fit procedure using voigt line shape applied after Shirley background subtraction [25] reveals five components related to the different chemical environments of silicon. The first component positioned at 99.2 eV corresponds to the emission from the elemental silicon demonstrating a 0.1 eV shift towards higher binding energy due to the final state effect in silicon clusters caused by a delay in the relaxation time of the photohole as compared to the time of the photoelectron emission. The clusters remain positively charged after the photoelectron emission process thereby decreasing its kinetic energy due to Coulomb interactions. The relaxation time and hence the loss in kinetic energy depends on cluster size as $1/r$, therefore existing cluster size distribution leads to the broadening of the Si^0 component so it appears as a single peak and the 2p doublet structure cannot be resolved. The components related to the Si^{n+} oxidation states are displaced with respect to the Si^0 line on 0.95, 1.85, 2.55 and 3.95 eV with full width at half maximum (FWHM) of 1.05, 1.15, 1.23 and 1.61 eV for $n=1-4$, respectively, which are close to values reported by Kim et al. [26] on a similar system. The relative concentrations of silicon oxidation states for normal and ultrasound-assisted implantation are given in Table 1. It is easy to see that *in situ* applied ultrasound treatment results in a substantial decrease of oxidation state concentrations whereas the intensity of the Si^0 state is about the same for all samples indicating that a nearly equal amount of silicon is precipitated.

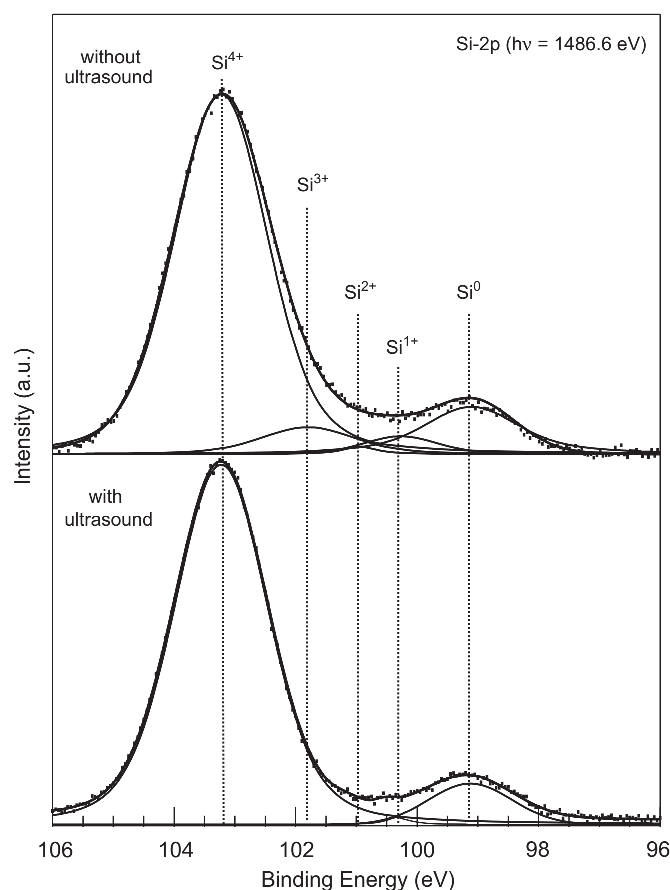

Fig. 2. High-resolution Si-2p photoemission spectra acquired on BHF-etched Si-implanted SiO_2 samples after annealing. The bottom spectrum corresponds to the measurement on sample implanted without applied ultrasound and the top spectrum corresponds to the measurement on the sample implanted with *in situ* applied ultrasound (acoustic power is 1.0 W/cm²).

Table 1
Relative integrated intensities of silicon oxidation states in implanted samples after annealing as revealed by fit of the photoemission spectra.

	Si^0(%)	Si^{1+}(%)	Si^{2+}(%)	Si^{3+}(%)	Si^{4+}(%)
With ultrasound (1.0 W/cm²)	9.5	1.0	0.0	0.0	89.5
Without ultrasound	9.6	3.3	1.5	6.2	79.3

An unambiguous assignment of the origin of the suboxide states is rather challenging. It is well known that ion irradiated silicon dioxide becomes substoichiometric and ultrasound treatment might result in additional modification of the silicon dioxide matrix, similar to the case of the implantation of metals [20,21]. However in our case, the suboxide states are detected only at the depth of maximum distribution of silicon particles and are absent below R_p, at the early steps of the etching process, assuming that high-temperature annealing leads to the complete annihilation of the irradiation-induced defects in the matrix. Furthermore, XPS depth analysis of SiO_2 layers irradiated with 130 keV Ar^+ ions at doses of $1-4\times10^{16}\,cm^{-2}$ and subjected to similar annealing conditions has not revealed any suboxide states as well. Taking this into account and comparing the amount of precipitated silicon with the amount of implanted silicon, we suggest that the majority of the measured states stem from the interface between silicon nanocrystals and silicon dioxide matrix as previously reported by Hadjisavvas et al. [27,28] and experimentally measured by Kim et al. [26].

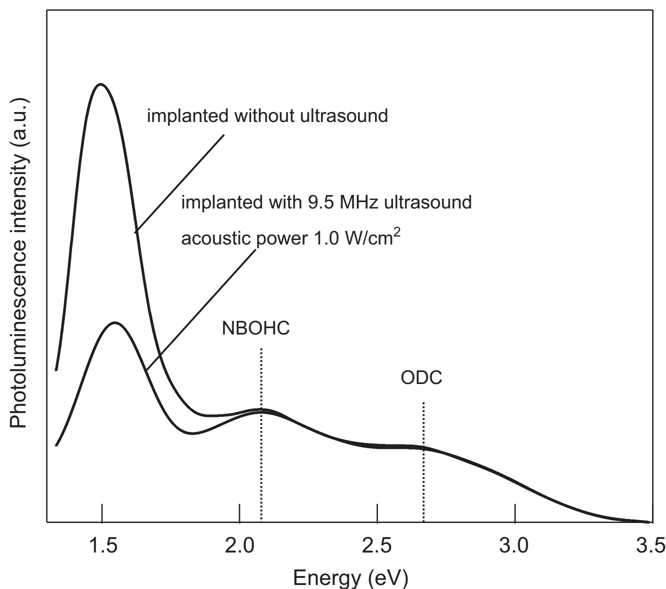

Fig. 3. Photoluminescence spectra measured on samples after annealing. The positions of emission bands related to nonbridging oxygen hole centers (NBOHC) and oxygen deficient centers (ODC) are marked with dashed lines.

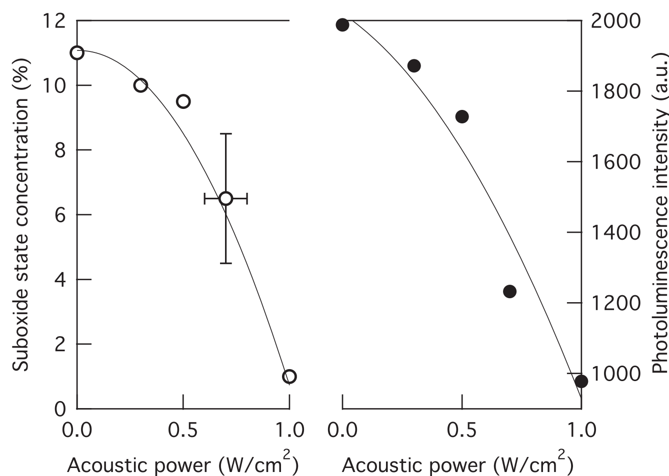

Fig. 4. Dependence of the total silicon suboxide states concentration (left) and photoluminescence intensity of the 1.5 eV photoluminescence band (right) on the applied acoustic power.

In Fig. 3 the corresponding photoluminescence spectra are presented. Both spectra possess a similar shape and consist of three bands located at about 1.5, 2.08 and 2.67 eV. The emission bands at 2.08 and 2.67 eV stem from the defects in the Si-implanted SiO_2 and are assigned to the nonbridging oxygen hole centers (NBOHC) [29] and oxygen deficient centers (ODC) [30], respectively, whereas the emission at ~1.5 eV is related to the crystallization of silicon. Whereas the defect band intensities are roughly the same, the 1.5 eV-band is markedly weaker in the sample implanted with applied ultrasound. Fig. 4 demonstrates the dependence of the total concentration of the silicon suboxide states Si^{n+} ($n = 1-3$) (left) and photoluminescence intensity of the 1.5 eV-band (right) on the applied acoustic power. The intensity of the 1.5 eV-band decreases with an increase in acoustic power suggesting correlation to the decreased concentration of the suboxide states. Taking into account that the average cluster size remains unchanged and cluster size distributions vary only slightly with an acoustic power, it can be inferred that the origin of the 1.5 eV-band is related to the suboxide states. Obtained results agree qualitatively well with theoretical calculations of Degoli [31] who studied presence of oxygen vacancies at the nc-Si/SiO_2 interface and give strong evidence to the light emission mechanism associated with the radiative states on the nanocrystal–oxide interface.

4. Conclusions

In summary, we have shown that ultrasound treatment applied during the implantation of silicon in silicon dioxide results in lower concentration of the suboxide states suggesting the formation of Si nanoclusters with a distinctly sharper nc-Si/SiO_2 interface. It was found that the behavior of the 1.5 eV photoluminescence band shows a strong dependency on the concentration of the suboxide states demonstrating an intensity increase with an increase in the state concentration. Thus, the presented results provide confirmatory evidence for the importance of the nc-Si/SiO_2 system chemistry and are essential in understanding light emission mechanisms in nanosized silicon.

Acknowledgments

Financial support by the Swiss National Foundation and the Swiss Federal Office of Energy is gratefully acknowledged. We also acknowledge the ion implantation group members (Institute of Semiconductor Physics, Kiev), in particular G. Kalistyi and V. Fedulov and thank R. Steiner (University of Basel) for technical support and S. Grözinger (University of Ulm) for TEM sample preparation.

References

[1] L.T. Canham, Appl. Phys. Lett. 57 (1990) 1046.
[2] A.G. Cullis, L.T. Canham, Nature 353 (1991) 335.
[3] O. Bisi, S. Ossicini, L. Pavesi, Surf. Sci. Rep. 38 (2000) 5.
[4] L. Pavesi. D.J. Lockwood (Eds.), Silicon photonics, in: Topics in Applied Physics, vol. 94, Springer, Berlin, 2004.
[5] S. Schuppler, S.L. Friedman, M.A. Marcus, D.L. Adler, Y.-H. Xie, F.M. Ross, T.D. Harris, W.L. Brown, Y.J. Chabal, L.E. Brus, P.H. Citrin, Phys. Rev. Lett. 72 (1994) 2648.
[6] Z.H. Lu, D.J. Lockwood, J.-M. Baribeau, Nature 378 (1995) 258.
[7] Y. Kanemitsu, T. Ogawa, K. Shiraishi, K. Takeda, Phys. Rev. B 48 (1993) 4883.
[8] M. Luppi, S. Ossicini, Phys. Rev. B 71 (2005) 035340.
[9] R.J. Baierle, M.J. Caldas, E. Molinari, S. Ossicini, Solid State Comm. 102 (1997) 545.
[10] M.V. Wolkin, J. Jorne, P.M. Fauchet, G. Allan, C. Delerue, Phys. Rev. Lett. 82 (1999) 197.
[11] A. Puzder, A.J. Williamson, J.C. Grossman, G. Galli, Phys. Rev. Lett. 88 (2002) 097401.
[12] B. Garrido, M. Lopez, O. Gonzalez, A. Perez-Rodriguez, J.R. Morante, C. Bonafos, Appl. Phys. Lett. 77 (2000) 3143.
[13] Q. Zhang, S.C. Bayliss, D.A. Hutt, Appl. Phys. Lett. 66 (1995) 1977.
[14] J.U. Schmidt, B. Schmidt, Mater. Sci. Eng. B 101 (2003) 28.
[15] L.A. Nesbit, Appl. Phys. Lett. 46 (1985) 38.
[16] C.F. Lin, W.T. Tseng, M.S. Feng, J. Appl. Phys. 87 (2000) 2808.
[17] T. Orii, M. Hirasawa, T. Seto, Appl. Phys. Lett. 83 (2003) 3395.
[18] T. Shimizu-Iwayama, K. Fujita, S. Nakao, K. Saitoh, T. Fujita, J. Appl. Phys. 75 (1994) 7779.
[19] K.S. Min, K.V. Shcheglov, C.M. Yang, H.A. Atwater, M.L. Brongersma, A. Polman, Appl. Phys. Lett. 69 (1996) 2033.
[20] A. Romanyuk, V. Spassov, V. Melnik, J. Appl. Phys. 99 (2006) 034314.
[21] A. Romanyuk, P. Oelhafen, R. Kurps, V. Melnik, Appl. Phys. Lett. 90 (2007) 013118.
[22] A. Romanyuk, P. Oelhafen, R. Steiner, P. Nellen, J. Reiner, V. Melnik, Surf. Sci. 595 (2005) 35.
[23] V.A. Burrows, Y.J. Chabal, G.S. Higashi, K. Raghavachari, S.B. Christman, Appl. Phys. Lett. 53 (1988) 998.
[24] I. Stenger, B. Gallas, L. Siozade, S. Fisson, G. Vuye, S. Chenot, J. Rivory, Phys. E 38 (2007) 176.
[25] D.A. Shirley, Phys. Rev. B. 5 (1972) 4709.

[26] S. Kim, M.C. Kim, S.-H. Choi, K.J. Kim, H.N. Hwang, C.C. Hwang, Appl. Phys. Lett. 91 (2007) 103113.
[27] G. Hadjisavvas, P.C. Kelires, Phys. Rev. Lett. 93 (2004) 226104.
[28] E. Lioudakis, A. Othonos, G. Hadjisavvas, P.C. Kelires, A.G. Nassiopoulou, Phys. E 38 (2007) 128.
[29] R. Tohmon, Y. Shimogaichi, H. Mizuno, Y. Ohki, K. Nagasawa, Y. Hama, Phys. Rev. Lett. 62 (1989) 1388.
[30] L. Skuja, Solid State Comm. 84 (1992) 613.
[31] E. Degoli, S. Ossicini, Surf. Sci. 470 (2000) 32.